Modification of the ICP Algorithm for Detection of the Occlusal Area of Dental Arches

Krzysztof Skabek and Agnieszka Anna Tomaka

Abstract We focused on the the process of finding the occlusal area of dental arches. The algorithm for detection of the occlusion area has been proposed. It is based on the ICP method that iteratively finds the best matching of two sets of points. The introduced method was discussed and compared to manually found occlusions and also to another methods.

Keywords 3D segmentation · Surface models · Dental arches · Occlusion detection · ICP algorithm

1 Introduction

In dentistry occlusion is defined as contact between teeth [4]. This contact may occur in many positions during chewing or at rest, but a significant role is attributed to maximum intercuspation—a person's habitual bite, called intercuspation position [6, 9]. As far as occlusion conditions influence the maxilla-mandible relation, and occlusion disorders may cause temporomandibular dysfunctions, evaluation of occlusion is one of the basics examinations in diagnosis of bruxism and other temporomandibular joint disorders [1]. Occlusion evaluation can be done directly by intraoral examination or using dental models, and nowadays it can be performed using computerized virtual dental models or segmented cone beam computed tomography (CBCT). Detection of the intercuspation position is then very important, as techniques of occlusion registration are prone to errors due to finite thickness of a wax bite, difficulties in intraoral scanning of teeth in occlusion and segmentation problems from CBCT with teeth in occlusion.

From a technical viewpoint the detection of intercuspation position is similar to a surface matching task, but in computer vision this matching problem is solved

K. Skabek (✉) · A.A. Tomaka
Polish Academy of Sciences, Institute of Theoretical and Applied Informatics,
BałTycka 5, Gliwice, Poland
e-mail: kskabek@iitis.pl

E. Piętka et al. (eds.), *Information Technologies in Medicine*,
Advances in Intelligent Systems and Computing 471,
DOI 10.1007/978-3-319-39796-2_9

for surfaces which have a common overlapping) area, for example scans of the same object from different viewpoints. The most popular technique of registration of such surfaces is the iterative closest point (ICP) algorithm. As the overlapping area is initially unknown the ICP algorithm, assuming the correspondence between matching surfaces as the closest points in actual position, finds the transformation minimizing distance between those points, and iteratively determines the position in which the distance is smallest. In this approach matched surfaces are treated as different views of the same object so intersections are not important. In ICP occlusion detection, however, surfaces of upper and lower teeth represent two complementary objects and direct application of ICP matching algorithm would yield the result in which corresponding points are at the closest position, but surfaces would intersects, which would not correspond to reality due to a collision of real objects.

We prepared technical assumptions for optimal occlusion from observations of tomographic imaging of the natural occlusion. It was stated a prerequisite of keeping the bone structure in non-collision space. Another assumption was also taken that we minimize the contact area on the top surface of dental arches.

In previous work we presented the method for finding the occlusion using a genetic algorithm minimizing a specially prepared energy function [10]. In this chapter we propose another approach based on statistical fitting of geometric structures. We used the ICP algorithm [3] which incrementally approximate the optimal fitting of two point sets. The transformation parameters R and T are estimated. Additionally, we assigned weights for each point of the structure to limit the area of searching.

2 Data Structures

2.1 Mesh and Oriented Point Representation

In the chapter we use mesh structures to represent surfaces. The meshes are obtained using scanning devices (such as Konica-Minolta VI-9i) in form of ordered points constructing the triangle mesh. Such mesh structure consists of a table of vertices V with normals N and topology F:

$$V = \{v_1, v_2 \dots v_k\} = \{(x_1, y_1, z_1) \dots (x_k, y_k, z_k)\}, \tag{1}$$

$$N = \{n_1, n_2 \dots n_k\} = \left\{(x_{n_1}, y_{n_1}, z_{n_1}) \dots (x_{n_k}, y_{n_k}, z_{n_k})\right\}, \tag{2}$$

$$F = \{f_1, f_2 \dots f_l\} = \{(v_1(f_1), v_2(f_1), v_3(f_1)) \dots (v_1(f_l), v_2(f_l), v_3(f_l))\}. \tag{3}$$

The topology of the mesh is stored as a set of triangles F and the triangles f_i are represented by three ordered indices $(v_1(f_i), v_2(f_i), v_3(f_i))$ pointing to the table of vertices V.

In our approach we use vectors normal to the vertices. They are calculated from normal vectors of topologically adjacent faces or, if there is no topological structure given, using PCA method of neighbouring points treated as a tangent plane [5].

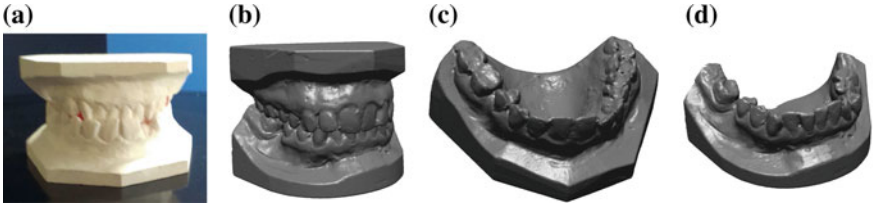

Fig. 1 Data for processing: **a** plaster dental models, **b** setting the correspondence with the wax bite, **c** digitalized model of the jaw, **d** Digitalized model of the mandible

2.2 Dental Models

In our application basic data for processing has the form of 3D triangle meshes which are digitalized 3D images of dental models. Such virtual dental models are obtained by digitizing plaster dental models (Fig. 1a) using a Konica-Minolta 3D scanner. Virtual models of the maxilla (Fig. 1c) and mandible (Fig. 1d) are created. Additional scanning of models with a wax bite enables establishing relation of both models in such a way that maps natural relation of maxilla and mandible (Fig. 1).

The technique of dental model scanning consists of several stages: data acquisition, registration of partial scans from different viewpoint merging them into a model and finally the structure processing [11]. Set of 24 partial scans is taken into consideration, 3 groups of 8 scans per model are acquired. Scans are merged in groups and then integrated. The obtained surface model needs some structure adjusting. Abnormal faces are found and corrected. Holes in the surfaces are also filled and if they are large, additional scanning which covers the artefacts is performed.

3 Algorithm for Finding the Occlusal Area

Our approach is based on the ICP algorithm [2, 3]. The routine minimizes the root square distance as a goodness function for two sets of points: the model point set $\mathbf{Q} = \{q_1, q_2 \ldots q_N\}$ and the input point set $\mathbf{P} = \{p_1, p_2 \ldots p_N\}$. The expression can be formulated as follows:

$$E = \sum_{i=1}^{N} ||\mathbf{R}p_i + T - q_i|\,|^2, \tag{4}$$

where $\mathbf{R}$ and T are rotation and translation of the point set.

The input data is not in correspondence with the model mesh so the first step of ICP algorithm is finding it.

3.1 Stages

There are several stages of the classical ICP algorithm [8]: (1) selection, (2) matching, (3) weighing, (4) rejecting, (5) measuring a distance error, (6) minimization of error metric.

3.2 Point-to-Plane Minimization

We use point-to-plane minimization as an optimization of the given mesh matching [7]. The matching measure is given as follows:

$$E = \sum_{i=1}^{N} ((\mathbf{R}\mathbf{p_i} + \mathbf{T} - \mathbf{q_i}) \cdot \mathbf{n_i})^2, \tag{5}$$

where $\mathbf{n_i}$ is normal in point p_i. We assume that for small angles the rotation matrix can be linearized:

$$\mathbf{R} = \mathbf{R_z}(\gamma)\mathbf{R_y}(\beta)\mathbf{R_x}(\alpha) \approx \begin{bmatrix} 1 & -\gamma & \beta \\ \gamma & 1 & -\alpha \\ -\beta & \alpha & 1 \end{bmatrix}. \tag{6}$$

3.3 Discrimination Measures

In our case there are two structures to be matched: first of them (denoted as $\mathbf{p}$), the upper jaw, is fixed and the second one (denoted as $\mathbf{p}'$), the mandible, is movable. To provide a better selection of structures which are important in the process of matching we introduced weights for the vertices. We establish the assumptions for the relative layout of the matching structures in form of a normalized weight measure. The weight measure consists of three components: $\sigma(\mathbf{p})$—the slope of corresponding vertices with regard to the fixed normal (7), $\rho(\mathbf{p})$—the slope of normals for corresponding vertices (8) and $D(\mathbf{p}, \mathbf{p}')$—the signed distance measure (9). The aim of the measure is to assign scalar values from the interval $[0 \ldots 1]$ to the vertices of the input mesh as weights $W(\mathbf{p})$ that discriminate less important parts in the matching process.

We calculate the dot product $\sigma(\mathbf{p})$ to obtain the direction of occlusion as expression:

$$\sigma(\mathbf{p}) = \vec{\mathbf{p}'\mathbf{p}} \cdot \mathbf{N}_{\mathbf{p}'}, \tag{7}$$

where: $|\mathbf{p}'\mathbf{p}| = d$ and $\mathbf{N}_{\mathbf{p}'}$ is normal vector at the point $\mathbf{p}'$.

Another measure which we considered is the relevance of normals at points $\mathbf{p}$ and $\mathbf{p}'$. This value is calculated from the expression:

$$\rho(\mathbf{p}) = \mathbf{N}_{\mathbf{p}} \cdot \mathbf{N}_{\mathbf{p}'}, \tag{8}$$

where: $\mathbf{N}_{\mathbf{p}}$ and $\mathbf{N}_{\mathbf{p}'}$ are normal vectors at the corresponding points $\mathbf{p}$ and $\mathbf{p}'$.

Third measure relates to the distance between two directed surfaces. It can be specified as a signed distance as follows:

$$D(\mathbf{p}, \mathbf{p}') = \mathbf{p} \cdot \mathbf{N}_{\mathbf{p}} - \mathbf{p}' \cdot \mathbf{N}_{\mathbf{p}}. \tag{9}$$

The resultant weight $W(\mathbf{p})$ can be specified for each vertex in two ways:

$$W(\mathbf{p}) = \left(1 - D(\mathbf{p})^2\right) \cdot th_0\left(\rho(\mathbf{p})\right) \cdot th_{\alpha > \alpha_0}(\sigma(\mathbf{p})), \tag{10}$$

$$W(\mathbf{p}) = \alpha(1 - D(\mathbf{p})^2) + \beta\, th_0(\rho(\mathbf{p})) + \gamma\, th_{\alpha > \alpha_0}(\sigma(\mathbf{p})), \tag{11}$$

where $th_i(x)$ is a threshold function:

$$th_i(x) = \begin{cases} x & \text{if } x \geq i, \\ 0 & \text{if } x < i. \end{cases} \tag{12}$$

Each component function $D(\mathbf{p})$, $\rho(\mathbf{p})$ and $\sigma(\mathbf{p})$ is normalized in equations (10) and (11). Parameters α, β and γ help to adjust the influence of the component values so the formula (11) is more flexible, but also needs additional adjustments and final normalization.

The influence of the components on particular mesh weight is illustrated in Fig. 2. Vertices with heavy weight are marked red, intermediate are coloured in gray or black, and those with weight of zero are omitted.

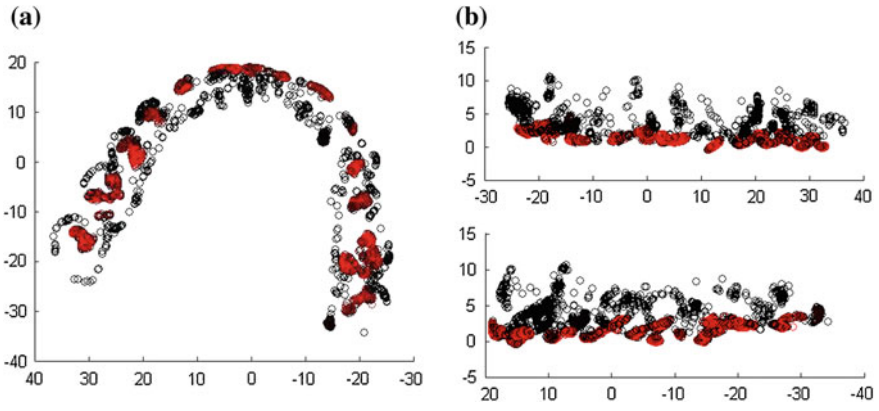

Fig. 2 Weights for ICP

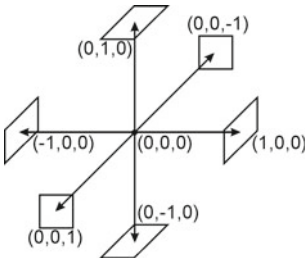

Fig. 3 Unit directions for the final correction

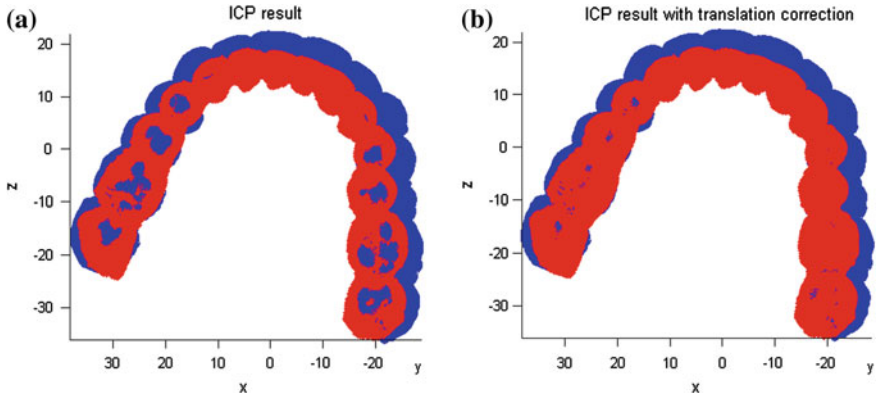

Fig. 4 Occlusion: **a** output of ICP with weights, **b** output of ICP with weights and correction

3.4 Final Correction

The correction ensures physical gap between the maxilla and the mandible. It is done by translating the mandible in 6 unit directions (see Fig. 3) to eliminate the overlapping structures. The set of translation vectors can be also extended to 26 items considering the intermediate directions. The correction is done incrementally assuming the minimum step ($\delta = 0.01$ mm in our case). The adjustment stops when all overlapping structures are eliminated or the current position yields a locally minimal overlapping (Fig. 4).

4 Testing the Occlusions

4.1 Contact Points

In Fig. 5a was shown the surface distribution of contact areas for dental arches within the range 0–1 mm after determination of the occlusal surface with the described

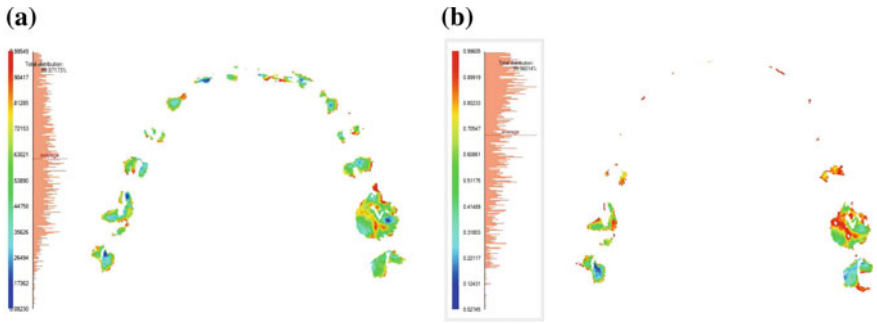

Fig. 5 Occlusion—contact points: **a** determined using the algorithm, **b** determined from CBCT

algorithm. A darker blue color indicates the actual contact places of the teeth. For comparison, Fig. 5b shows the contact area of the teeth in their anatomical position acquired from CBCT imaging.

Contact points and fitting surfaces are also visible in the image of cross sections taken along a circle with center in the middle of the reference structure and the rotation axis OY. The characteristic phases of cross-sections with the contact area are shown in Fig. 6.

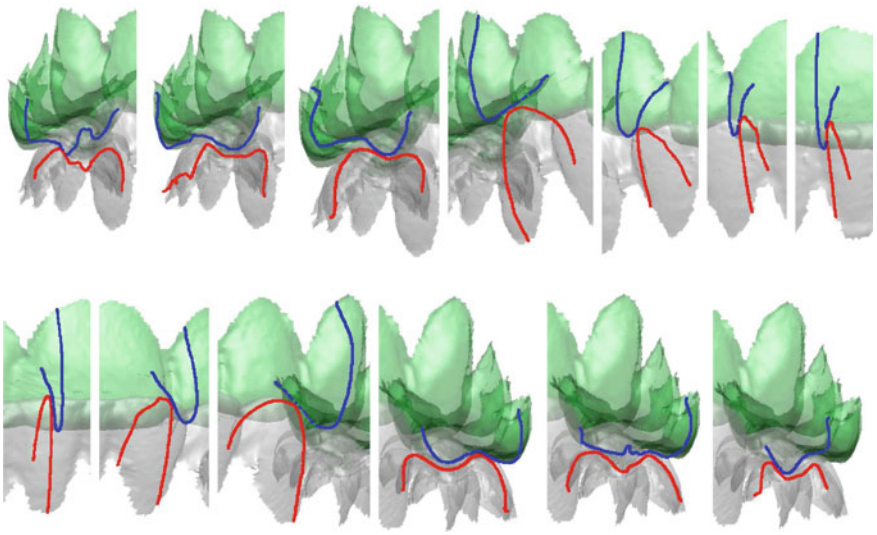

Fig. 6 Occlusion—cross sections

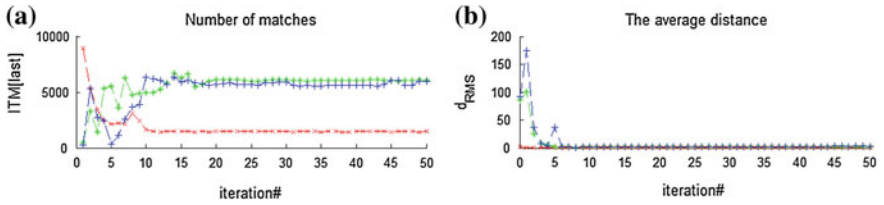

Fig. 7 Stability analysis for three cases (50 iterations): **a** the number of matched items, **b** the average distance

4.2 Stability of the Algorithm

We tested the stability of the aligning algorithm with weights. Experiments were performed in 50 iterations. It turned out that the convergence of the algorithm stabilized after a few iterative steps (Fig. 7). The effect of the initial position on the stability of matches was tested. The fastest convergence was obtained for meshes initially brought into its center of gravity and matched principal components using PCA analysis (case 1 –x– red). Other cases were arranged with structures in the random initial position: translation (case 2 –+– blue), and also translation and rotation (case 3 –*– green).

4.3 Comparison to Practical Cases

We analyzed three kinds of natural occlusions: occlusion from CBCT, occlusion from face scanning, occlusion from dental models.

The best fit was obtained for the 3D scan of plaster models in the fixed position. Several stable points of support can be distinguished in this case. The average distance error with regard to the proposed method was 0.222 mm and standard deviation 0.181.

A similar situation occurred in the case of occlusion obtained from CBCT imaging. The average error distance was, in this case, 0.334 mm and standard deviation 0.632. Comparison of the two cases is shown in Fig. 5.

The most significant differences were obtained for 3D face scan using an occlusal bite. Two distinct points of support were marked on the back molars and there was lack of support of anterior teeth. The results from our fitting method strongly differs from the position of the mandible in this case. The average distance error was 2.66 mm and standard deviation 1.917.

Table 1 Fitting distance errors and standard deviation for ICP and genetic methods with regard to natural alignment from CBCT imaging

ICP1		ICP2		Genetic1		Genetic2	
d_{err}	std_{dev}	d_{err}	std_{dev}	d_{err}	std_{dev}	d_{err}	std_{dev}
0.222	0.181	0.303	0.396	0.217	0.191	0.252	0.187

4.4 Comparison to Other Methods

In the chapter [10] was described another method considering the usage of genetic algorithms with a given optimization formula to find the area of occlusion for two compatible jaws.

After the comparison to the fitting errors obtained by the genetic algorithm, it turned out that the results lead to even smaller differences. The results are given in Table 1.

Moreover, the advantage of genetic method is the application of the objective measure, relevant to the quality of fitting. Unfortunately, disadvantage is the long processing time and much smaller convergence of the optimization process.

5 Conclusions

Finding the occlusal surface is an important part of determining the spatial relationship between the upper and lower dental arch. The process involves the search matches between the natural tooth cavities between the bumps.

The search can be limited to neighborhoods with direct contact friction between the teeth. The chapter selected such surfaces and gave them appropriate weights, greater than the others. In contrast, areas not involved in occlusion were rejected, they were given the importance of zero.

An algorithm for matching the occlusal surface using a method ICP was developed. The algorithm determines the contact surface of teeth by calculating the averaged position of the suitably weighted friction surfaces of the mandible relative to the maxilla. The last step of the algorithm determines the transformation that minimizes the contact area between the two dental arches.

The quantitative convergence of the cases was analyzed by comparing the calculated occlusion area with the positions of the natural occlusion and that obtained by the use of a genetic minimization algorithm.

The next steps were provided to improve the methods of determining the occlusal surface constraints and to optimize the energy function for the genetic algorithm. The genetic approach seems to be promising because of the availability of an objective energy function for surface fitting.

The possible use of the described methods includes the determination of the occlusal surface in the design of occlusal splints for the treatment of bruxism.

Acknowledgments This work was supported in part by the National Science Center, Poland under the research project 2012/07/B/ST6/01238.

References

1. Baron, S.: Bruxism and occlussion. In: Palla, S., Kato, T., Provaznik, I., Tkacz, E., Baron, S. (eds.) Novel Methodology of Both Diagnosis and Therapy of Bruxism, Lecture Notes of the ICB Seminar, 137th Seminar, Warsaw (2014)
2. Besl, P.J., McKay, N.D.: A method for registration of 3-D shapes. IEEE Trans. Pattern Anal. Mach. Intell. **14**(2), 239–256 (1992)
3. Chen, Y., Medioni, G.: Object Modeling by registration of multiple range images. In: Proceedings of IEEE Conference on Robotics and Automation (1991)
4. Davies, S., Gray, R.M.J.: Practice: what is occlusion? Br. Dent. J. **191**(5), 235–245 (2001)
5. Hoppe, H., DeRose, T., Duchamp, T., McDonald, J., Stuetzle, W.: Surface reconstruction from unorganized points. Comput. Graphics **26**(2), 71–78 (1992)
6. Mah, J., Hatcher, D., Harrell, W.: Craniofacial imaging in orthodontics. In: Graber, L., Vanarsdall, R., Vig, K. (eds.) Orthodontics: Current Principles and Techniques, ISBN: 032306641, 2012, 5th edn. Mosby, Elsevier (2012)
7. Pomerleau, F., Colas, F., Siegwart, R.: A review of point cloud registration algorithms for mobile robotics. Found. Trends Robot. **4**(1), 1–104 (2015)
8. Rusinkiewicz, S., Levoy, M.: Effcient variants of the icp algorithm. In: Proceedings of Third International Conference on 3-D Digital Imaging and Modeling, pp. 145–152 (2001)
9. Sander, F.: Analiza modeli (Model analysis). In: Diedrich, P. (ed.) Ortodoncja I, Rozwój struktur ustno-twarzowych i diagnostyka (Orthodontics I, Development of Bucco-Facial Structures and Diagnosis), ISBN: 83-89581-85-X, (in Polish). Wydawnictwo Medyczne Urban & Partner, Wrocław (2004)
10. Skabek, K., Tomaka, A.A.: Techniques of processing and segmentation of 3D geometric models for detection of the occlusal area of dental arches. In: Palla, S., Kato, T., Provaznik, I., Tkacz, E., Baron, S. (eds.) Novel Methodology of Both Diagnosis and Therapy of Bruxism, Lecture Notes of the ICB Seminar, 137th Seminar, Warsaw (2014)
11. Tomaka, A.A.: Analiza obrazów wielomodalnych dla potrzeb nieinwazyjnej diagnostyki ortodontycznej (Multimodal Image Analysis for Noninvasive Orthodontic Diagnosis). ISBN: 978-83-62652-46-4, (in Polish), IITIS PAN (2013)